Luminescence of Cr^{2+} Centres and Related Optical Interactions Involving Crystal Field Levels of Chromium Ions in Zinc Sulfide *

G. Grebe

Institut für Festkörperphysik der Technischen Universität Berlin

and H.-J. Schulz

Institut für Elektronenmikroskopie am Fritz-Haber-Institut der Max-Planck-Gesellschaft, Berlin-Dahlem

(Z. Naturforsch. **29 a**, 1803–1819 [1974]; received September 27, 1974)

In the i.r. emission of ZnS:Cr crystals, a zero-phonon doublet at 5211 and 5216 cm^{-1} and a number of vibronic bands are resolved at $T \approx 4$ K. The T_d symmetry of the crystal field at the Cr^{2+} ion on a Zn lattice site is reduced to D_{2d} by a static Jahn-Teller effect. Differences in the vibronic structures of absorption and emission indicate prevalence of quasi-local vibrations in the spectra. An exponential decay of the i.r. luminescence in the μs range yields an oscillator strength $f = 6 \times 10^{-4}$ ($T = 4$ K) in accordance with selection rule reasoning for the radiative transition $^5A_1(^5E) \rightarrow {}^5B_2(^5T_2)$.

By interrelating a fit of transmission spectra with excitation spectra of luminescence and photoconduction, the distance of the Cr^{2+} centres from the conduction band edge is evaluated at 20700 cm^{-1} ($T = 300$ K). An irradiation of the crystals with photons of energies above this optical ionization threshold causes a sensitization for the Cr^{2+} i.r. luminescence. Thus, apart from effects related to traps, a novel excitation band at 10500 cm^{-1} arises which is interpreted by the $^6A_1(^6S) \rightarrow {}^4T_1(^4G)$ transition of Cr^+ centres. This transition terminates in a level degenerate with conduction band states so that free carriers will be released which, in turn, induce the Cr^{2+} emission.

Furthermore, at some of the crystals, the i.r. emission between 2500 and 3000 cm^{-1} of Fe^{2+} centres is recorded with the best resolution obtained so far.

1. Introduction

Whereas the optical properties of a series of transition metals in II-VI compounds have been investigated for a long while now, Chromium as an optically active centre was found only in 1961: At CdS:Cr crystals and ZnS:Cr crystals, an absorption $^5T_2 \rightarrow {}^5E$ at the split ground state ^5D of Cr^{2+} was found [1]. However, after preceding optical excitation, e.p.r. signals of Cr^+ centres could be recorded, this so for example at ZnS [2], CdTe [3] as well at ZnSe [6] and at ZnS [7]. All e.p.r. results confirm observed for the first time at CdS [5] and later also at ZnSe [6] and at ZnS [7]. All. e.p.r. results confirm the original assumption that Cr is incorporated on a cation site. For the visible luminescence in ZnS, Chromium (as well as Fe, Co, and Ni) acts as a killer [8].

At the same time, an emission of ZnS:Cr in the near infrared was found which was interpreted as an electronic transition $^5E(^5D) \rightarrow {}^5T_2(^5D)$ [9, 10]. The absorption structure of Cr^{2+} for ZnS [7, 11] and other host lattices [7] was studied in detail and thus a fine structure of zero phonon lines and vibronic bands was revealed. Of all known iron group impurity centres in II-VI compounds, Cr^{2+} centres are the only ones which, in their ground state, are subject to a static Jahn-Teller effect. Therefore, particularly from the fine structure found in emission at low temperatures [12], further informations should be accessible on the ground state **.

On a cation lattice site, Cr^{2+} – an ion of $3d^4$ electron configuration – is located in a crystal field of T_d symmetry. For this case, Dunitz and Orgel [13] postulated a static Jahn-Teller effect which leads to a strong compression of the tetrahedron in the directions of its three twofold symmetry axes. Thus, as a function of the normal coordinates Q_2 and Q_3 (cf. [14]) potential surfaces with three equivalent minima are obtained. The resulting tetragonal symmetry group in D_{2d}; the threefold orbitally degenerate $^5T_2$ ground state splits further. Figure 1 de-

* Requests for reprints should be addressed to Priv.-Doz. Dr. H.-J. Schulz, Institut für Elektronenmikroskopie am Fritz-Haber-Institut der Max-Planck-Gesellschaft, *D-1000 Berlin 33*, Faradayweg 4–6.

** The present paper comprises results of the doctoral thesis by G. Grebe, Fachbereich Physik der TU Berlin, D 83 (1974).

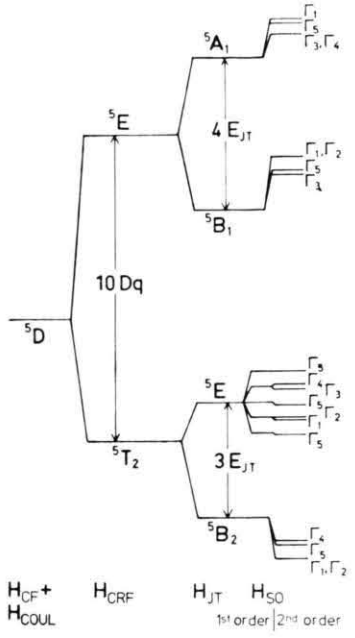

Fig. 1. Level splitting scheme of the ^5D state of Cr^{2+} ions in ZnS.

monstrates this splitting (cf. [15]) as well as spin-orbit interaction for the ground state $^5T_2$ and the excited ^5E state on the assumption of D_{2d} symmetry (according to [7]). The Jahn-Teller coupling, or E_{JT} respectively, will be different for the two states. The representations of the resulting terms are given by the decomposition of the irreducible representations of T_d to those of D_{2d}. By means of this symmetry reduction to D_{2d} earlier e.p.r. measurements at Cr^{2+} in II-VI compounds can be interpreted (cf. [14], p. 169).

The five orbital states given by the representations of group D_{2d} are still at $S = 2$ fivefold spin degenerate each. If the spin-orbit coupling is a small perturbation, the representations of the spin-orbit terms are obtained by reduction of the product of the irreducible representations of the orbital and of the spin functions, respectively. Apart from $^5E(^5T_2)$, these terms split only by 2nd order spin-orbit interaction or by spin-spin coupling (cf. [16]).

2. Experimental Procedures

2.1 Equipment and Methods

Emission spectra were recorded with an evacuated grating spectrometer (1 m, Jarrell-Ash), using gratings with 295 lines/mm (blazed at 2.6 μm) and with 600 lines/mm (blazed at 1.6 μm). The i.r. emission was excited by a xenon high pressure arc lamp which illuminated the crystal either from the surface turned towards, or turned away from, the spectrometer. The crystal was cooled in a helium immersion cryostat [17], in some cases at reduced helium vapour pressure. For the radiation detection cooled or uncooled PbS photoconductors were used. The optical beam was chopped with low frequency and the obtained a.c. signal was detected by means of a lock-in amplifier system.

With a similar equipment, however using an iodine-tungsten lamp, absorption measurements were made. Transmission spectra were obtained by a digital point-by-point analysis of the recorder traces. The atmospheric water vapour absorption was taken into account by subtraction. Some absorption measurements at 300 K were recorded with a double-beam grating spectrometer (Bausch & Lomb) in the wave number range between $\bar{\nu} = 15000\ cm^{-1}$ and $\bar{\nu} = 30000\ cm^{-1}$.

In the excitation measurements a double monochromator (Zeiss MM 12) was used with an iodine-tungsten lamp or a xenon high pressure arc lamp as radiation sources. The excitation spectra were recorded by adjusting the radiation for constant power in the covered spectral region. This was done by controlling the slit widths of the monochromator. In some measurements, the crystal was excited by the unchopped illumination of an additional light source, e.g. a mercury high pressure arc lamp. Also in the excitation measurements, the radiation emitted from the crystal was detected by an equipment similar to the one mentioned above.

Photoconduction spectra [18] were mainly studied at 80 K and at 300 K. At 25 K, only some tentative measurements were made because the recording of reproducible spectra was aggravated by space charge effects. For conductivity measurements, either contacts of "Leitsilber" were applied or indium electrodes which had been evaporated or soldered ultrasonically. A prism single monochromator (Leiss) or interference filters were used for the spectral selection. Additional excitation was possible so that photoconduction spectra could be recorded also with sensitized crystals.

For decay experiments, a ruby laser (Holobeam 300) was available with a pulse width of 10 ns and a decay time constant of some ns. The infrared luminescence excited at 14403 cm^{-1} was detected by a thermoelectrically cooled InAs photocell (Philco-Ford, IAT 704) whose time constant was determined to $\tau = 0.6\ \mu s$. The photovoltage signal was amplified (Hewlett-Packard, 462 A wide band amplifier), displayed on an oscilloscope, and photographed.

Tab. 1. Impurities of the crystals A, B, and C. In the qualitative analysis, higher concentrations are denoted by "++", "n.d." means: not detectable. The limits of sensitivity vary here for the elements marked by n.d. from 2 ppm (Co, Ni) to 20 ppm (B); for Sc, this limit is unknown. In the quantitative analysis, all numbers are given in parts per million (ppm). The symbol "<" is used where no calibration samples had been prepared.

	crystal	B	Mg	Si	Ca	Cr	Mn	Fe	Cu	Ag	Cd	other elements
Qualitative Analysis	A	+	++	++		+	++	++	+	++		n.d.: Sc, Ti, V, Co, Ni
	B	n.d.	+	+		++	+	+	+	+		
Quantitative Analysis	A		<30	<100	<10	30	n.d.	30	4	25	n.d.	n.d.: Ge, In, Sn, Sb, Au, Pb, Bi
	B		< 3	<100	<10	400	n.d.	10	2	5	<200	
	C		< 3	<300	<30	900	n.d.	1	5	n.d.	n.d.	

2.2 Crystals

The experiments were performed mainly with three typical samples which had been synthetized in different production procedures:

Crystal A was grown in the Institut für Festkörperphysik, TU Berlin, by the iodine-transport technique from a mixture of ZnS powder, $CrCl_3$, and a small amount of S. The ampoule had been positioned in a temperature gradient of 750° to 950 °C.

Crystal B was grown from the melt at Eagle-Picher Industries.

Crystal C was grown in the hydrothermal procedure at the Aerospace Research Labs., Wright-Patterson AFB, Ohio.

The crystals have been examined as to their impurities by spectrographic analysis (Table 1). First, small fragments of crystals A and B were checked qualitatively (BAM, Berlin). A quantitative analysis (TH, Eindhoven) was carried out on small sections of crystals A and C and for crystal B on an adjacent piece from the same melt.

An examination of the double-refraction with a polarization microscope yielded crystal A being cubic and crystal B having about 15% hexagonal structure.

3. $Cr^{2+}(3d^4)$ Transitions

3.1 Infrared Emission

The emission spectra in the range of 4000 to 5250 cm^{-1} (Fig. 2) differ for the three ZnS crys-

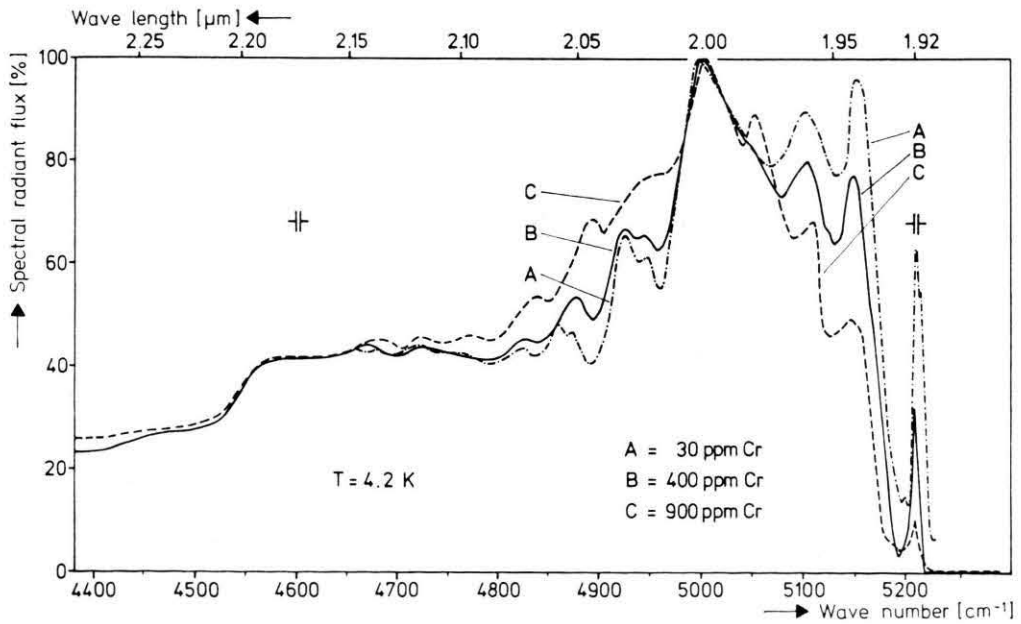

Fig. 2. Emission spectra of ZnS:Cr crystals of various origins and activator concentrations. Excitation range: $\tilde{\nu}=7700$ . . .40000 cm^{-1}. The spectra have been corrected for the spectral response characteristics of the PbS detector and the spectral efficiency of the grating and have been normalized at $\tilde{\nu}=5000$ cm^{-1}. Photon energies are given as vacuum wave numbers in this figure as well as in the following ones. Spectral slit widths are indicated.

tals A, B, and C which are described more detailed in Section 2.2.

Near 5215 cm^{-1}, the spectrum shows a doublet of zero phonon lines whose half width is about 5 cm^{-1}. They are distinctly resolvable at crystals A and B. With wave numbers $\bar{\nu} \leqq 5200\ cm^{-1}$, a wide range characterized by vibronic structures is annexed to the zero phonon lines. The separable bands show half widths $\Delta\bar{\nu} \geqq 50\ cm^{-1}$.

At crystal A, the zero phonon lines have maxima at $(5210.7 \pm 0.3)\ cm^{-1}$ and $(5215.9 \pm 0.3)\ cm^{-1}$. The given limit of error was derived from the scattering of the measured values. The distance of the two lines is $(5.3 \pm 0.1)\ cm^{-1}$. The intensity ratio of these two lines does not change if the temperature is lowered from 4.2 K to 2.9 K (Figure 3). However, at 77 K the lines have disappeared. With crystal A, the two lines prove to be polarized only very weakly or not at all.

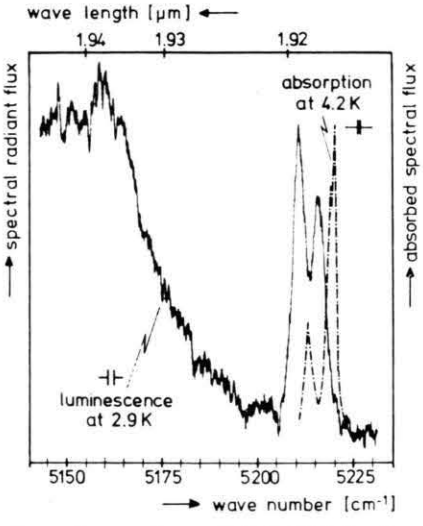

Fig. 3. Zero phonon lines of $ZnS:Cr^{2+}$ in the emission spectrum of crystal A ($T = 2.9$ K), and in the absorption spectrum of crystal B ($T = 4.2$ K).

The corresponding emission lines at crystal B have energies of $(5212.0 \pm 0.5)\ cm^{-1}$ and $(5216.8 \pm 0.5)\ cm^{-1}$. Compared with crystal A they are displaced to higher energies by about 1 cm^{-1}.

3.2 Infrared Absorption

Absorption measurements at ZnS:Cr crystals were published in 1970 by Kelley and Williams [11] and by Vallin et al. [7]. In these papers, the spectra differ in the structure of absorption near 5200 cm^{-1} and in the positions of absorption bands around 8400 cm^{-1} and 11000 cm^{-1}. In order to examine the intensities of the zero phonon lines and the overall shape of the absorption with the crystals discussed here, measurements were made between 4000 cm^{-1} and the band edge of ZnS at about 30000 cm^{-1}.

Apart from a broad unstructured absorption maximum at about 6000 cm^{-1}, the zero phonon range near 5200 cm^{-1} is particularly remarkable (cf. Figure 3). Whereas at crystals B and C the absorption is well resolvable, it is only just detectable at crystal A. A measurement * at crystal B was plotted in Fig. 3 after applying the corrections explained in Section 2.1. The maxima of the absorption lines (half width $\Delta\bar{\nu} \approx 3\ cm^{-1}$) are at $(5213.7 \pm 0.1)\ cm^{-1}$ and at $(5219.9 \pm 0.1)\ cm^{-1}$, the given limit of error indicating again the scattering between the various measurements. Thus, the doublet in absorption is displaced by about 2 to 3 cm^{-1} at crystal B compared to the doublet in emission. In absorption, at crystal B the doublet is also either polarized only very weakly or not at all. At crystals B and C, some further sharp absorption lines are found which are distinctly polarized: at 5174, 5179, 5180, and 5183 cm^{-1} as well as at 5125 cm^{-1} for crystal C only. These lines correspond to the "hexagonal" lines in the mentioned papers [7, 11] of other authors.

3.3 Interpretation of Absorption and Emission: $3d^4$ Ground State Splitting (Quintet System)

3.31 Zero Phonon Lines

As pointed out in the Introduction (cf. Fig. 1), the $^5B_2$ ground state of the Cr^{2+} centres splits into three levels by spin-orbit coupling. The Γ_5 term is situated above the Γ_1, Γ_2 ground state with a distance of 3 D. D was defined in [19] and determined as $D = -(1.77 \pm 0.02)\ cm^{-1}$ from e.p.r. measurements at ZnS:Cr. This result means that the Γ_5 term is situated above the ground state in a distance of $3|D| = (5.3 \pm 0.1)\ cm^{-1}$, and, correspondingly, the Γ_4 term folowing next at $4|D| = (7.1 \pm 0.1)\ cm^{-1}$. The measured separation in the emission doublet suggests to associate these two lines with transitions from the same initial state into these terms. It remains to investigate which terms of the excited state can be regarded as the initial level for these emission transitions.

* carried out by M. Wöhlecke, at that time III. Physikalisches Institut der TU Berlin.

Both transitions begin in a state which originates from the $^5E(^5D)$ term. According to the selection rules in D_{2d} symmetry, electric dipole transitions into the $^5B_2$ ground state are allowed from $^5A_1$ but not from $^5B_1$ (cf. [20], Table 13).

The emission transitions will originate mainly from the lowest spin orbit level Γ_3, Γ_4 ($^5A_1$) from which electric dipole transitions are allowed to Γ_1, to Γ_2 and to Γ_5. Transitions to the highest spin-orbit state Γ_4 of the $^5B_2$ ground state should, therefore, not occur. This interpretation is well confirmed by the agreement between the experimental distance of 5.3 cm^{-1} of the two zero phonon lines in emission (crystal A) on the one hand, and the distonce of 5.3 cm^{-1} between the Γ_1, Γ_2 ground state and the Γ_5 term evaluated by Vallin et al. [7, 19] on the other hand.

The absorption measurements support the given interpretation: at 4 K the intensity of the absorption line at 5214 cm^{-1} is smaller than that at 5220 cm^{-1}; the intensity of the former increases with increasing temperature at the expense of the line with higher energy [7]. Due to the temperature rise, more Cr^{2+} centres with occupied Γ_5 resp. Γ_4 states are available for the absorption. At the same time, the number of centres with occupied Γ_1, Γ_2 ground states decreases.

The line doublet in absorption has a separation of 6.2 cm^{-1}; with respect to the corresponding emission lines, the two absorption lines are shifted to higher energies by 2 . . . 3 cm^{-1}. These observations, too, can be interpreted in the level scheme of the Cr^{2+} centres. The fact that a doublet is found also in absorption means that both transitions terminate in the same state. In D_{2d} a number of electric dipole transitions are allowed between the spin-orbit states of the $^5B_2$ term and those of the excited $^5A_1$ term (cf. [20], Table 13). Hence the conclusion that the spin-orbit splitting of the $^5A_1$ term is so small that it cannot be resolvet in absorption (cf. [7]). The energy difference of the two transitions is then equal to that between the Γ_1, Γ_2 ground state and the Γ_5 resp. Γ_4 term of $^5B_2$. The distance between Γ_5 and Γ_4 with $D = 1.8$ cm^{-1} is too small to be resolved so that the transitions from the two latter terms are recorded as one absorption line in the spectrum. The distance of this line with respect to the line originatin from the Γ_1, Γ_2 ground state is accordingly larger by about 1 cm^{-1} than the distance of the two zero phonon lines in emission.

The small energy displacement of the two lines between emission and absorption can be interpreted in the same way. The spin-orbit states of the $^5A_1$ term represent a certain energetic width of the term, even if they are closely neighboured. Unlike the emission transitions which mainly originate from the low energy Γ_3, Γ_4 level, absorption transitions also lead to the higher spin-orbit states. Thus, the absorption lines are slightly shifted towards higher energies.

The ratio of the absorption constants of the distinctly polarized "hexagonal" absorption lines between 5125 cm^{-1} and 5183 cm^{-1} to those of the "cubic" lines near 5220 cm^{-1} clearly differs from that of [11]. This modification and the spectral position of the "hexagonal" lines prove a polytype structure of crystals B and C.

3.32 Vibronic Bands

According to Laporte's selection rule, electric-dipole transitions between d-states are parity-forbidden. For two reasons this restriction is not strictly valid: (1) There is no inversion centre in T_d symmetry. The restriction is violated by an admixture of odd-parity states, for instance p-states mixed into d-states. (2) By coupling of phonons, the selection rule is lifted to an extent that depends on temperature. On these grounds, an emission spectrum is observed whose intensity distribution is mainly determined by vibronic transitions (cf. Figure 2).

The energy differences between the zero phonon emission and the maxima of the vibronic bands are given in Table 2.

Tab. 2. Vibronic emission bands of ZnS : Cr^{2+}

zero phonon line cm^{-1}	vibronic peaks cm^{-1}	wave number difference cm^{-1}	remarks
5210	5150	60	
	5105	105	
	5050	160	crystal C
	5000	210	main peak
	4925	285	crystals A and B
	4870	340	crystals (A and) B
	4850	360	crystal A

The relative intensities of the various bands depend on the Cr concentration. In particular, the two phonon bands in a distance of 60 cm^{-1} and 105 cm^{-1} from the zero phonon emission decrease with increasing chromium concentration relative to

the main band at 210 cm^{-1} distance. Whereas in emission the vibronic maximum is displaced by 210 cm^{-1} from the zero phonon doublet, in absorption the displacement is about 500 cm^{-1}. The vibronic spectrum in emission is structured by individual distinct bands. However in absorption only weak shoulders and peaks occur on a broad spectrum ($\Delta\bar{\nu} \approx 1000$ cm^{-1}).

Vallin et al.[7] have tried to derive from the absorption spectrum arguments for the presence of a minute Jahn-Teller coupling in the excited state. Therefore, in model C of these authors the $^5E(^5D)$ term is not split. They start from the assumption that the $^5B_2$ state is situated lower than the non-split $^5T_2$ state by E_{JT}. According to the term system given by these authors[7], the stabilization energy is, however, $2\,E_{JT}$.

If one seeks to interprete the structure of the vibronic spectra on the basis of one of the five models A ... E in[7], each model yields that the maxima of the vibronic absorption and emission would have to be shifted by the same amount of energy with respect to the zero phonon lines. This conclusion disagrees with the experimental results given in the present paper. Moreover, the argumentation of Vallin et al.[7] suggests that their models lead to a Jahn-Teller energy which is at best as high as the shift between vibronic and electronic emission. With our results thus follows $E_{JT} \leqq 200 \ldots 250$ cm^{-1}. According to[21] this result is not compatible with the prerequisite of a strong Jahn-Teller coupling which leads to the tetragonal distortion. Taking as a basis the model of Fig. 1, this energy would even be bisected.

Hence, the attempt[7] to derive the term structure of the excited state from the vibronic absorption spectrum leads to results which are not compatible with the emission spectra described in this paper. The suggested interpretation according to which the excited state is split by the Jahn-Teller effect either very weakly or not at all does no longer seem to be sufficiently justified.

Interpreting the structure of the vibronic emission spectrum, two cases must be considered: 1st, the phonons coupled to the transitions are phonons of the undisturbed ZnS lattice. 2nd, the coupling phonons are vibrations affected by the impurity centre.

At first, the spectra are compared with the known values of the ZnS phonons at the critical points of the Brillouin zone and with the density of states distribution of the phonons[22]. The phonon density of states is still low at the energy difference of 60 cm^{-1} found here; this number is still below the value TA(L) $\approx$ 70 cm^{-1}. This comparison and also the occurrence of a maximum in the emission spectrum at this place lead to the interpretation that vibrations influenced by the Cr^{2+} centres couple to the electronic transition. The emission maximum near 105 cm^{-1} falls into the energy range of the TA branch at the points X and K. Since, however, the density of states is of low value and moreover does not peak here, this vibronic emission maximum must also be interpreted as a quasi-local vibration. The maximum with a difference of about 160 cm^{-1} which is only distinctly pronounced at crystal C could result from a summation of the two phonons just described. Further, the main maximum at about 210 cm^{-1} can be interpreted as the sum of two phonons with 105 cm^{-1}. A coupling of several local phonons to an electronic transition which includes a level with Jahn-Teller effect is known[14]. For pure ZnS, LA(X) $\approx$ 210 cm^{-1}, it is true, but here, again, a small density of states is found. The vibronic emission at wave numbers $\bar{\nu} \leqq 5000$ cm^{-1} corresponds to maxima of the phonon density of states which concur with the TO branch and the LO branch. It can, therefore, be interpreted as a coupling with such phonons of the optical branches of ZnS.

Thus, the most pronounced vibronic structures of the emission spectrum cannot be traced back to phonons of the ZnS lattice. There are neither T_2 nor the E-mode phonons of the undisturbed lattice which had, in particular, there are no E-mode phonons of the undisturbed lattice as had been used for the interpretation of the structure of the vibronic absorption spectrum[7]. At present, the interpretation proposed here does not allow conclusions on the symmetry of the Cr^{2+} centres. However, the different structures of the absorption and emission spectra can be interpreted. In the excited state the interaction with the lattice is different from that in the ground state. This leads to different vibrational modes in the two states which determine the vibronic emission resp. absorption. A future quantitative treatment is intended of the vibronic energy levels of the Cr^{2+} ground state including the Jahn-Teller effect.

3.4 Excitation Spectrum: Higher Levels (Triplet System)

Interpreting the i.r. emission and absorption as electronic transitions at the split ground state ^5D, the higher terms of the Cr^{2+} ions and the position of the ground state within the ZnS energy band model have, as yet, always been set aside. The higher terms of Cr^{2+} ions were determined by Tanabe and Sugano [23] in the approximation of a strong crystal field. In contrast to the quintet ground state they are singulets and triplets. Inter-combination transitions with their low oscillator strengths entail a low absorption and are thus often only detectable by excitation measurements.

Excitation of the i.r. emission of Cr^{2+} centres is possible in a wide spectral range (Fig. 4). Near the band edge, a broad excitation band at about 23000 cm^{-1} dominates the spectrum; in this range also

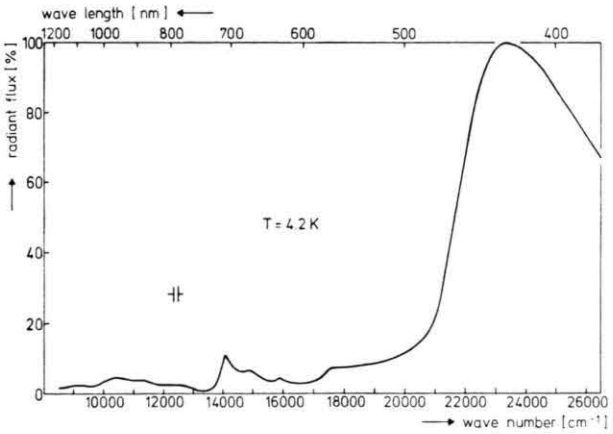

Fig. 4. Excitation spectrum of the ZnS: Cr^{2+} infrared emission (crystal C). Detectable emission range: $\tilde{\nu} = 3400 \ldots 6500\ cm^{-1}$.

photoconduction can be excited (see Section 4). The various excitation bands of low intensity in the spectral range of 8000 cm^{-1} to 20000 cm^{-1} [24] are, however, not to be found in the photoconduction spectrum. In the mentioned paper [24], the authors demonstrated how to interprete those bands by electronic transitions to higher terms of the Cr^{2+} ions in the crystal field. Such transitions are spin-forbidden but this interdiction need not be strictly applied in the case of spin-orbit interaction. The spin-restriction does explain, however, the low excitation probability in relation to the excitation band near 23000 cm^{-1} and to the excitation within the quintet term system. These latter transitions lead to a broad range of good excitability around 6000 cm^{-1} which turns up again in the absorption spectrum as a wide band (cf. Section 3.2). Application of the crystal field approximation on the excitation spectrum allows to determine the crystal field parameter Dq and the Racah parameters B and C by means of the Tanabe-Sugano matrices [23]; the elements of these matrices depend on these parameters. The results [24] $Dq = 510\ cm^{-1}$, $B = 500\ cm^{-1}$, $C = 2850\ cm^{-1}$ is based upon a fit starting with the excitation band at 14100 cm^{-1} which is characterized by both, small half width and horizontal course of the corresponding level in the Tanabe-Sugano diagram.

The Dq of 510 cm^{-1} resulting from the computational fit is – within the expected accuracy – in very good agreement with the value from emission and absorption measurements. Basing a simple crystal field approximation on the zero phonon transition $^5T_2 \longleftrightarrow {}^5E$ which was found in emission and absorption at 5215 cm^{-1}, i.e. equalizing this energy with $10\,Dq$, the value $Dq \approx 520\ cm^{-1}$ results. The determination of Dq in this approximation is however, dubious in so far as the Jahn-Teller effect splits the ^5E and $^5T_2$ states, as described, and thus involves deviations in the Dq value. In this approximation Dq numbers for Cr^{2+} can be determined from absorption measurements at other II-VI compounds: Dq varies from 500 cm^{-1} at CdSe [25] and CdTe [26] up to 555 cm^{-1} at ZnSe [27].

Tab. 3. Racah parameters of the free Cr^{2+} ion.

B cm^{-1}	C cm^{-1}	Reference
810	3565	Tanabe and Sugano 1954 [23]
845	3690	Catalan et al. 1954 [28]
830	3430	Griffith 1964 [29] (p. 437)

Since no comparable optical data are available, an examination of B must be based on the B value of the free Cr^{2+} ion (Table 3). The value obtained for B is about 60% of the value in the free ion. It is in good agreement with the corresponding data at other II-VI compounds. The reduction of B can be regarded as resulting from the extension of the charge cloud of the d-electrons due to partial covalency of the bond (cf. [30], p. 88). Consideration of covalency contradicts the presumptions of the crystal field approximation. The reduction of the

Racah parameters B and C takes this deviation into account. In the literature [22, 31, 32] for ZnS, ionicities are reported between about 60% and 80%. The found reduction factor of appr. 0.8 for C also matches with the indicated range. Due to the disparity of the reduction factors for B and C, the ratio C/B increases here to 5.7 whereas usually it lies between 4 and 5. This value can still be regarded as satisfactory if one considers the very simplified conditions on which the term energies were calculated.

In spite of the good overall agreement with the excitation spectrum – especially as regards the number of the bands – there are some points which need to be clarified. This is particularly true for the deviation of the $^3T_2(^3H)$ level from the measured value at 11000 cm^{-1}. In the preceding paper [24] a stronger configuration interaction had been proposed at this term to effect this reduction.

In the calculations, the band at 12550 cm^{-1} corresponds to the energy of the $^1A_1$ term. Transitions from the $^5T_2$ ground state into this excited state are, however, very unlikely (cf. [29], p. 305) since for them $\Delta S = 2$. Moreover, these transitions are configuration-forbidden (cf. [33], p. 116) since two electrons would have to flop from t_2 states to e-states. Nevertheless, in our spectra a weak excitation band at 12550 cm^{-1} is distinguishable.

3.5 Decay of Cr^{2+} Emission

At crystals B and C, the decay curves of the Cr^{2+} i.r. emission were recorded at 4.2 K, 77 K, and 300 K. The crystals were excited by means of a laser with $\bar{\nu} = (14403 \pm 3)\,cm^{-1}$. The emission was measured with an InAs detector using germanium as a filter or sometimes using an interference filter ($\bar{\nu}_{max} = 4993$ cm^{-1}, half width $\Delta\bar{\nu} = 155$ cm^{-1}). The decay curves are, in good approximation, exponential function from which time constants were taken in semi-logarithmical plots. The time constants were corrected with those of the photocell, of the amplifier, and of the oscilloscope. The decay time constants obtained decrease monotonically with increasing temperature (Table 4).

Tab. 4. Decay time constants (in μs) of the ZnS: Cr^{2+} infrared emission
a) without
b) with
} interference filter (see text).

T	crystal B		crystal C	
	a	*b*	*a*	*b*
4 K	7.7	7.1	8.7	8.1
77 K	7.1	7.0	7.9	7.6
300 K	5.3	5.4	4.9	4.7

Provided that two-step processes can be neglected, the excitation by means of a ruby laser leads to an excitation of the i.r. emission without simultaneously causing photoconduction, i. e. without involving the energy bands of the crystal. Electronic processes within a centre have a mono-molecular reaction kinetics, as has been observed here.

As mentioned in Section 3.32, electric-dipole transitions are parity-forbidden among the pure d-states of the Cr^{2+} ion. The absence of an inversion centre in T_d symmetry leads, however, to a mixing of the 3d states with 4p states, i. e. to an admixture of odd-parity states which is even intensified by the symmetry reduction to D_{2d}. The covalency of the ZnS lattice also causes a reduction of the decay time constants [34].

The found time constants depend – to a small degree – on the temperature (cf. Table 4). The reason is that the parity interdiction holds strictly only for $T = 0$. With increasing temperature this restriction is, however, lifted more and more by lattice vibrations. For electric-dipole transitions in a crystal field without a centre of inversion, which are not strictly forbidden in the first place because of 3d-4p mixture, a small decrease of the time constant with temperature will result. Also as a consequence of covalency, the emission decays more rapidly with increasing temperature [35].

The oscillator strengths can be calculated (cf. [36]) from the decay time constants:

$$f = \frac{m\,c^3}{2\,e^2\,\omega^2}\left(\frac{E_c}{E_{eff}}\right)^2 \frac{A}{n}$$

where E_c the average electric field in the crystal,

E_{eff} the electric field at the ion,

n the index of refraction,

ω the angular frequency of the photon.

E_c/E_{eff} can also be determined [37] from the index of refraction. With $n = 2.26$ [22], $(E_c/E_{eff}) = 3/(n^2+2) = 0.42$. If there are no competitive radiationless processes, the decay time constant $\tau = A^{-1}$ directly renders the Einstein coefficient A and thus the oscillator strengths: $f = 6 \times 10^{-4}$ at 4 K, and $f = 1 \times 10^{-3}$ at 300 K.

From absorption measurements $f = 5 \times 10^{-3}$ – a comparatively high value – was found for ZnS: Cr^{2+} [11].

The order of magnitude of f allows the conclusion that the decay is determined by spin-allowed transitions which have typical oscillator strengths of 10^{-4} (cf. [36], p. 415); spin-forbidden transitions however have oscillator strengths of $10^{-7} \ldots 10^{-8}$ (cf. [36], p. 415. [33], p. 116). The excitation of the infrared emission in these decay measurements should result from the transition $^5T_2(^5D) \rightarrow {}^3T_1(^3H)$, which is spin-forbidden, whereas the emission transition is spin-allowed. It might be speculated that in these experiments the i.r. emission was excited instead by transitions within the triplet system.

4. Photo-Ionization of Cr^{2+} Centres

4.1 Photoconduction

The excitation spectrum of Cr^{2+} i.r. emission (cf. Fig. 4) which is composed of intercombination bands in the spectral range $\bar{\nu} \leqq 20000\ cm^{-1}$ is dominated for $\bar{\nu} \geqq 21000\ cm^{-1}$ by transitions of distinctly higher oscillator strengths which are also found in the spectra of photoconduction and of absorption. The excitation spectra of photoconduction were measured at 25 K, 80 K * and 300 K * (Fig. 5) at a crystal from the same line of production as crystal B.

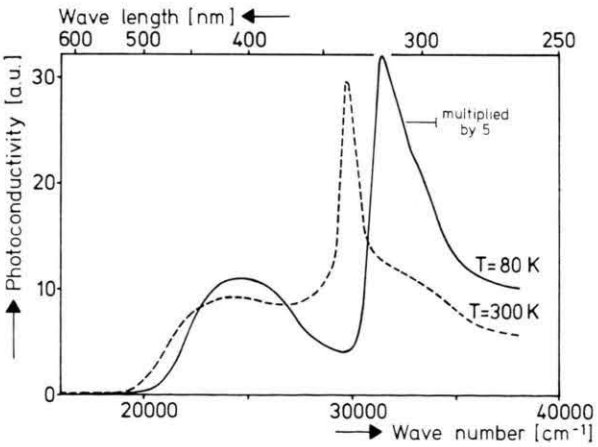

Fig. 5. Spectral response of photoconductivity; ZnS:Cr (100 ppm according to the producer) grown from the melt by Eagle-Picher Ind. as crystal B. The crystal had been converted into the "normal state" (see Section 5.1) before recording this response spectrum.

With decreasing temperature, the long wave cut-on threshold of the photoconduction shifts towards higher energies; at 25 K it reaches a value of about $\bar{\nu} \approx 20500\ cm^{-1}$.

* carried out by P. Wolter, at that time II. Physikalisches Institut der TU Berlin.

4.2 Excitation of I.R. Emission and Absorption

Measurements of absorption and excitation spectra in the region leading to photo-ionization were again made at crystals from the same production series as crystal B * and at crystal C at 4.2 K, 77 K and 300 K. The energy where the structured excitation region (cf. Fig. 4) merges into the broad excitation band, changes from 19500 cm^{-1} at 300 K to 21000 cm^{-1} at 4.2 K. At excitation in the range of $23000 \ldots 31000\ cm^{-1}$, the intensity of the i.r. emission is only moderately dependent on energy; it depends, however, on the temperature.

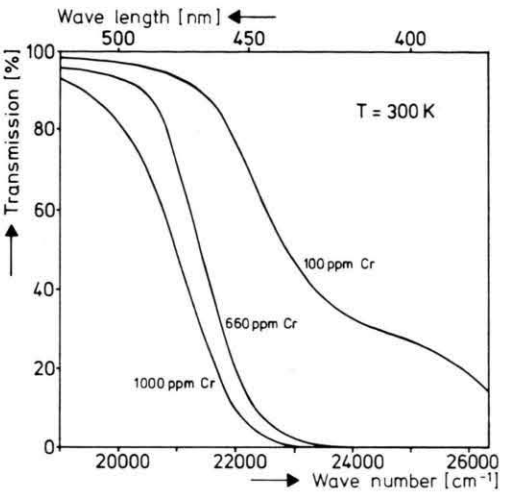

Fig. 6. Transmission spectra of three crystals with various Cr concentrations grown from the melt by Eagle-Picher Ind. as crystal B. Concentrations in the figure according to the producer. The background absorption has been subtracted.

In the transmission spectra (Fig. 6), too, one recognizes the low energy edge known from photoconduction spectra. Here, its shifting with concentration is to be seen. Eventually, only at the crystal of low doping a structure in the transmission at $\bar{\nu} \geqq 23000\ cm^{-1}$ is visible which is masked at higher doping levels.

4.3 Interpretation

The equal threshold energy derived from the absorption tail and from the photoconductive response allows the determination of the energy which is required for photoionization of the localized centres. Since ZnS is an n-type photoconductor, transitions from the Cr^{2+} centres to the conduction band must be involved – as far as other centres can be excluded. These transitions from the centres

to the conduction band are favoured above the spin-forbidden transitions within the Cr^{2+} so that no structure will be found in the broad absorption tail. On the other hand, the low-intensity intercombination bands of the Cr^{2+} could be masked by a strong transition from a different centre to the conduction band.

The photo-ionization of $3d^n$ impurities in semiconductors with zincblende structure is to be treated [38, 39] by investigating the matrix elements for electric dipole transitions between linear combinations of d-type one-electron wave functions – which can be mixed with p-states – and the continuum of states in the conduction band, i. e. Bloch functions. Particularly for t_2 states, the admixture of *p*-functions can be expected (cf. [40], p. 111). The conduction band is assumed to be parabolic.

Neglecting spin-orbit coupling and Coulomb interaction between the electron and the ionized centre, for the absorption constant α:

$$\alpha/h\nu \sim (1-\beta^2)\,(h\nu - E_i)^{3/2} + \beta^2\, E_p (h\nu - E_i)^{\frac{1}{2}}$$

where

$h\nu$ the photon energy,
E_i the ionization energy of the centre,
β the rate of admixture of 4p states to the 3d states, and
E_p = 21 eV for II-VI compounds (cf. [39]).

With $\beta = 0$, the expression $(\alpha/h\nu)^{2/3}$ plotted versus $h\nu$ yields a straight line which intersects the abscissa at E_i. The stronger the admixture of 4p states, the stronger can be expected the deviations from this straight line. They are, however, only noticeable for $\beta > 10\%$.

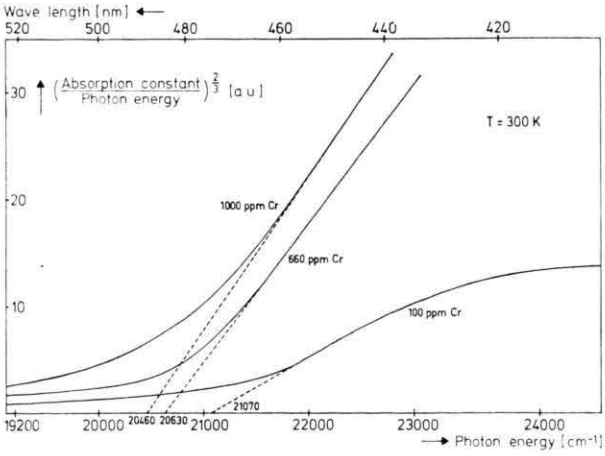

Fig. 7. Derivation of the photo-ionization energies by means of the transmission spectra given in Figure 6.

For three crystals of various Cr concentrations (Fig. 7), the linear parts of the described function have been extrapolated to $\alpha = 0$. The evaluation must be limited to a region in which a parabolic conduction band can be assumed, i. e. appr. $(h\nu - E_i) \leqq 2500\,cm^{-1}$. Indeed, within this region straight lines result. The intersections with the abscissa yield ionization energies 21070 cm^{-1}, 20630 cm^{-1}, and 20460 cm^{-1} for crystals with 100, 660, and 1000 ppm Cr, respectively.

The result shows that the assumptions of the theory [38] are fulfilled and thus, at 300 K, the ground state of the Cr^{2+} centres can be localized in a distance of $(20700 \pm 500)\,cm^{-1}$ from the bottom of the conduction band. The successful approximation of the transmission curves suggests a but small admixture of 4p states, in agreement with [40] and [41]. Also, $\beta < 10\%$ is well matching with the oscillator strengths of about 10^{-3} which were determined in Section 3.5 (cf. [41]).

Deviations of the converted transmission curves from linearity at low photon energies can be caused by transitions with phonon coupling [38]. However, the great width of the protruding absorption and the positive correlation with the Cr concentration rather suggest the inner transitions in the Cr^{2+} effective in this range to be the cause. The error in the determination of the ionization energy due to uncertainty of the background absorption is, however, small.

The identified ionization energy of about 20700 cm^{-1} fits reasonably well with the range of 18500 ... 20000 cm^{-1} for the position of a Cr^{2+} centre below the conduction band as determined [42] by means of crystal field theory assuming $Dq = 500$, $B = 550$, and $C = 2600\,cm^{-1}$. These numbers are again in good agreement with those determined for Cr^{2+} (cf. Section 3.4).

The temperature dependency of the threshold energy as has been observed here is comparable with the thermal variation of the band gap for ZnS which amounts to about 1200 cm^{-1} over the 4 to 300 K temperature range. Hence it can be concluded that the distance of the Cr^{2+} centres from the valence band is nearly independent of temperature.

4.4 Recombination of Freed Carriers

The processes discussed in Section 4 concern the photo-ionization of Cr^{2+} centres, i. e. a generation at these centres of quasi-free charge carriers. As

indicated by the strong band in the excitation spectrum in this region, recombination of the carriers again leads to infrared luminescence at Cr^{2+} centres. These processes are to be discussed in the following with taking into account that the Cr-doped crystals may also contain levels of other impurities or defects possibly lying deeper in the forbidden energy band.

On exciting the i.r. emission of the Cr^{2+} centres with $\bar{\nu} \geqq 20000\,cm^{-1}$, Cr^{2+} centres and presumably other activator centres A^- will be ionized so that Cr^{3+} centres and A centres will result:

$$Cr^{2+}(+h\nu) \rightarrow Cr^{3+} + e_c^-$$
$$A^- \ (+h\nu) \rightarrow A \ + e_c^-,$$

e_c^- = electron in the conduction band.

No references are given in the literature as to Cr^{3+} centres being stable in II-VI compounds. Pappalardo and Dietz[1] mention inner transitions at Cr^{3+} centres as a possible cause for an absorption of CdS:Cr near $10000\,cm^{-1}$. Moreover, the existence of Cr^{3+} centres has been used as a hypothesis for the interpretation of various experiments since then [43–46]; the presence of Cr^{3+} could, however, in no case, be proven without doubt.

This may be due to the plausible anticipation that Cr^{3+} ions incorporated tetrahedrally on ZnS lattice sites will have a high electron affinity and will therefore recombine rapidly with electrons. For this recombination, conduction electrons are eligible or even valence electrons if the ground state of Cr^{3+} is below the top of the valence band. In this latter case, secondary processes would occur.

Hence, the following mechanisms are possible for the excitation of Cr^{2+} i.r. emission by means of photo-ionization processes:

(a) $Cr^{3+} + e_c^- (+Cr^{2+}) \rightarrow (Cr^{2+} +)\,[Cr^{2+}]^*$

(b) $Cr^{3+} + e_v^- (+Cr^{2+}) \rightarrow (Cr^{2+} +)\,[Cr^{2+}]^*$

(c) $A^- \rightarrow A + e_v^-$

$A + e_c^- + Cr^{2+} \rightarrow A^- + [Cr^{2+}]^*$,

e_v^-: electron in the valence band.

Ref. a: The Cr^{3+} ion recombines with a free electron immediately after ionization. Thus, an excited Cr^{2+} centre $[Cr^{2+}]^*$ is created which (partly) releases its energy in the transition to the ground state by i.r. emission. The energy could also be transferred to another Cr^{2+} centre, as indicated by the symbols in round brackets.

Ref. b: If the Cr^{3+} ground state is situated low enough, in analogy to the process described under (a), also the recombination with a valence electron e_v^- is possible. As a consequence of this process, an activator centre A^- may acquire one positive unit charge if an electron from this centre recombines with a hole in the valence band.

Ref. c: If activator centres are ionized by the excitation as initially supposed or if A-centres ensue from the process described under (b), conduction electrons e_c^- will recombine with these centres. The released energy can lead to an excitation of Cr^{2+} centres and thus to i.r. emission.

The participation of the various processes in the excitation of the i.r. emission depends on temperature and on photon energy. An experimental indication is, for instance, furnished by the excitation spectrum where the region closely below the band gap has a temperature-dependent structure (see Section 4.2).

5. Interactions Involving $Cr^+(3d^5)$ Centres

5.1 Excitation of Infrared Emission with Simultaneous or Preceding Sensitization

An excitation spectrum as shown in [24] can always be recorded if the crystal has been converted into the "normal state". This means that the crystal must be annealed at a temperature $T \geqq 300\,K$ and must not be excited with radiation of $\bar{\nu} \geqq 21000\,cm^{-1}$ before the beginning of the measurement. At 300 K it takes several hours to reach the normal state, at 400 K it takes a few minutes only. At lower temperatures, the crystal can be turned back into this state by means of red irradiation (carried out with $\bar{\nu} \leqq 17000\,cm^{-1}$). Simultaneous or preceding blue irradiation, however, produces sensitized states of the crystal.

Thus, at $T = 4.2\,K$ a simultaneous irradiation in the region $\bar{\nu} \geqq 21000\,cm^{-1}$ effects a sensitization for the excitation in the range $\bar{\nu} \leqq 21000\,cm^{-1}$ (Figure 8). The excitation effected by the additional blue irradiation itself could be discriminated experimentally by not modulating the sensitizing blue irradiation, yet modulating, as usual, the exciting radiation. A comparison of Fig. 8 b with Fig. 8 a (corresponding to Fig. 1 of [24]) demon-

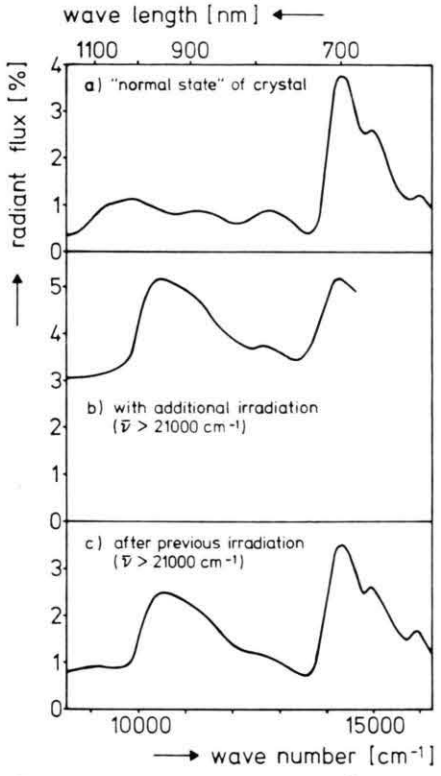

Fig. 8. Excitation spectra of the ZnS: Cr^{2+} infrared emission at $T=4.2$ K (crystal C) for the various "states" of the crystal. Detectable emission range: $\bar{\nu}=3400\ldots6500\ \mathrm{cm}^{-1}$.

strates 1st that the additional irradiation superimposes the structure of the normal excitation spectrum with a component essentially independent of wave numbers; 2nd it generates a new band in the spectrum at 10500 cm^{-1} which is also maintained after switching-off the additional irradiation.

On recording the peak intensity of this excitation band at 10500 cm^{-1} immediately after switching-off the additional blue irradiation, the band decays in the dark to a smaller height with a time constant of some minutes. This time constant is determined by the decay of the mentioned additive part of the excitation. During this measurement, the (modulated) excitation at 10500 cm^{-1} as a measuring probe is always only switched-on for a few seconds. With continued (modulated) excitation, however, the new excitation band would decay more rapidly and reach a smaller value.

After decay of the additive part, the excitation band produced at 10500 cm^{-1} remains stable in the dark over several hours at 4.2 K. An excitation spectrum recorded now (Fig. 8 c, cf. Fig. 4) still shows the new band situated in a position where the spectrum has a minimum in the normal state.

By intensive red irradiation (measured with $\bar{\nu}\leqq 17000\ \mathrm{cm}^{-1}$), the band can be quenched within 1 to 2 hours, and thus the normal state is restored. Hence, in particular an irradiation with $\bar{\nu}=10500\ \mathrm{cm}^{-1}$ causes a "self quenching effect". The additional red irradiation can, by the way, also lead to a temporary intensification of the 10500 cm^{-1} band during the decay of the band immediately after blue pre-irradiation.

At 4 K and at 80 K, a transient i.r. emission (range of measurement: $\bar{\nu}=3400\ldots6500\ \mathrm{cm}^{-1}$) can be stimulated by irradiation with $\bar{\nu}\leqq 21000\ \mathrm{cm}^{-1}$ if the crystal had been pre-irradiated with blue light ($\bar{\nu}\geqq 21000\ \mathrm{cm}^{-1}$). With switching-on the stimulating radiation, the i.r. emission increases to a maximum value (with the time constant of the amplifier) and then declines within a few minutes to the level corresponding to the power of the exciting radiation (spectral response: cf. Figure 8 c). After annealing at 250 K between initial excitation and stimulation, the i.r. emission flash shows up invariably on subsequent cooling though shallow electron traps of the crystals have been emptied by this treatment.

5.2 Discussion of Charge Transfer Processes

5.21 Emptying of Electron Traps

From thermo-luminescence measurements it is known that in ZnS by incorporation of Cr deep electron traps are produced at 5500 ... 8000 cm^{-1} (0.7 ... 1 eV) below the conduction band [8, 47–49]. In these thermo-luminescence experiments and in measurements of the thermally stimulated conduction at various Cr doped crystals [18] both, position and height of the glow maxima depend, to a great extent, on the selection of crystals. Apart from the electron traps, the glow spectrum is determined by the nature and the number of recombination centres, too. However, for the interpretation of the processes described here, properties of the electron traps are important which do not depend on the exact position of their energy levels. At weakly doped ZnS (60 ppm Cr), thermo-luminescence measurements at 80 K yield a minimum energy $\bar{\nu}=21500\ \mathrm{cm}^{-1}$ for filling the electron traps and a minimum energy of 8500 cm^{-1} for their emptying [49].

The measured increase of the i.r. emission at additional irradiation can, thus, be interpreted as a process of two partial steps: A blue d.c. light excitation with $\bar{\nu} \geqq 21000\,cm^{-1}$ continually produces electrons in the conduction band, as confirmed by the photoconduction spectra (cf. Section 4.1). Since a d.c. component of the i.r. emission cannot be detected, the only matter of interest here is that some of these free electrons will populate electron traps. A modulated radiation with an energy $\bar{\nu} \geqq 8000\,cm^{-1}$ re-empties the occupied electron traps. Hence, an additional modulated i.r. emission results due to the processes described in Section 4.4. This component of emission superimposes the emission originating from processes within the Cr^{2+} centres. The 133-Hz modulation employed here suggests the time constants of rise and decay of the optical emptying of traps being, at most, of the order of some ms. The given interpretation of the excitation spectra of the Cr^{2+} i.r. emission at additional irradiation can be corroborated by analogous processes in photo-conduction experiments [18].

An increase of the modulated emission at additional irradiation can, thus, be understood as an additive component of the total modulated emission. This part should not exhibit a marked spectral dependency since it is caused by transitions from traps to empty states of the conduction band. A complete independency from the excitation energy can, however, not be expected since the density of states in the conduction band and the trap distribution should become apparent.

Whereas in the above described processes filling and emptying of traps took place simultaneously, the stimulated i.r. emission flash and the analogous transient effect in the photoconduction show how filling and emptying of traps can be partially separated in time.

5.22 Inner Transitions and Charge Transfer Processes at Cr^{+} Centres

The interpretation of the processes of simultaneous or successive stimulation as described above was based on traps. Several authors have proven (e. g. [2, 50–52]) that in Cr doped ZnS Cr^{+} ions produce a centre which is detectable by e.p.r. To determine the energy depth of the Cr^{+} centre, so far frequently the method of glow experiments in luminescence [47, 48] or conductivity has been applied. By this method the Cr^{+} centre is being identified with the traps so that the mentioned depth of 0.7 ... 1 eV results. Comparative measurements of the e.p.r. signal of Cr^{+} and of the thermoluminescence [49, 53] have shown, however, that this identification is no longer justified. At ZnS crystals the traps turned out to lie in a depth of $4000 \ldots 8000\,cm^{-1}$ (0.5 ... 1 eV) below the conduction band. In addition, Cr^{+} centres appear in almost the same energy region but with a different kinetics. The excitation band at $10500\,cm^{-1}$ is closely related to these Cr^{+} centres, as will be substantiated now.

As is known [51], at 80 K Cr^{+} centres are produced in ZnS: Cr by irradiation with $\bar{\nu} \geqq 20000\,cm^{-1}$. Whereas at low temperatures the Cr^{+} e.p.r. signal decays with time constants of 3 ... 4 hours [53], it is rapidly quenched except for a small rest above 300 K [47, 53]. Cr^{+} centres can be quenched optically [47]; for this process, a minimum energy of $5000\,cm^{-1}$ is required [8].

A comparison of the e.p.r. experiments with the properties of the $10500\,cm^{-1}$ excitation band described in Section 5.1 proves an analogous behaviour for these two effects. To begin with, the question will be discussed whether the band at $10500\,cm^{-1}$ can be ascribed to a transition within the Cr^{+} ion. In order to estimate the transition energy we start from the Tanabe-Sugano diagram of the d^5 configuration. The value $B = 710\,cm^{-1}$ for the free Cr^{+} ion (cf. [29], p. 437) yields – with a covalency factor of 0.6 – the value $B = 430\,cm^{-1}$ in the crystal. Lowest in energy is the transition between the $^6A_1(^6S)$ ground state and the $^4T_1(^4G)$ term. Reasoning by analogy, the Dq value for Cr^{+} can be assumed smaller than the value for Cr^{2+} which has been determined above as $Dq \approx 500\,cm^{-1}$: suppose $Dq/B \approx 1$. Here, the distance of the mentioned terms in 25 B and, hence, the energy difference $\bar{\nu} \approx 11000\,cm^{-1}$. The value $C = 1950\,cm^{-1}$ for the Racah parameter $C = 4.5$ B implied by using the Tanabe-Sugano diagram is in sufficient agreement with the number evaluated from the free ion value [29] by considering the covalency. Thus, within the acquired accuracy, a notable agreement is found between the estimated transition energy and the position of the band maximum.

The intensity of this spin-forbidden excitation band is similar to that of the likewise spin-forbidden transition in Cr^{2+}. For the time being, one has to bear in mind that the energy of the excited Cr^{+}

can only lead to an excitation of the i.r. emission of a distant Cr^{2+} via some interposed energy transfer process.

After having treated the inner transitions in the $3d^5$ electron configuration of Cr^+, now transitions at this centre with participation of the bands will be discussed. Indeed, the optical quenching of the Cr^+ e.p.r. signal by radiation with $\bar{\nu} = 5000 \ldots 20000$ cm^{-1} and the quenching of the 10500 cm^{-1} excitation band suggest a photo-ionization of the Cr^+ centres. The transitions of electrons into the conduction band at this process are also detectable by the stimulated photoelectric current which decays with a comparable time constant [18].

A similar analogy turns out between the temperature dependencies in the thermal quenching both of the Cr^+ e.p.r. signal and of the 10500 cm^{-1} excitation band. Thus, a thermal quenching energy of appr. 0.7 ... 0.8 eV is inferred which fits quite reasonably the given minimum energy for optical quenching of the e.p.r. signal.

It follows that the excitation band at 10500 cm^{-1} is situated in a spectral region where transitions are possible from the Cr^+ to the conduction band. It is thus comprehensible that this excitation band decays more rapidly immediately after pre-irradiation with continuous excitation at 10500 cm^{-1} than in the case where the crystal is kept in the dark.

The appearance of the additional excitation range around $\bar{\nu} = 10500$ cm^{-1} as a band and, moreover, its slight asymmetry suggest transitions to excitation states of the Cr^+ centres which are degenerate with conduction band states [54]. The resulting generation of conduction electrons by absorption in the sensitized excitation band would now easily explain the subsequent i.r. emission by means of the process (c) discussed in Section 4.4. Whereas this mechanism takes place at distant A-centres, the possibility of recombination at the same Cr centre must not be excluded.

With this interpretation, the temporary increase of the excitation band at 10500 cm^{-1} by additional red irradiation can be understood which occurs if the traps of the crystal had been filled by blue excitation before. The additional red irradiation empties the "fast" traps into the conduction band. The simultaneously proceeding slow ionization of the Cr^+ centres is, thus, transitorily superimposed by the formation of additional Cr^+ centres so that the excitation band increases temporarily, before the quenching dominates.

One could try to associate the excitation band at 10500 cm^{-1} with Cr^{3+} centres in ZnS. However, the above mentioned kinetic arguments and estimates of the energy differences based on crystal field theory tell against a (meta)stable presence of such centres [1].

An effect similar to the sensitization of ZnS:Cr was also reported for ZnS:Co, Cu where a very broad band with a maximum at 10500 cm^{-1} occurs both in the excitation spectrum of the Co^{2+} i.r. emission and in the absorption spectrum [55]. Furthermore, an additional absorption is present near 10000 cm^{-1} at electroluminescent ZnS:Cu, Cl crystals [56] and an interpretation in terms of transitions from the valence band to Cu^{2+} centres is given. In the present case, a relation of the additional excitation band at 10500 cm^{-1} to some intrinsic lattice defect should not be excluded though the interpretation in terms of a Cr^+ transition seems to be fairly convincing.

6. $Fe^{2+}(3d^6)$ Transitions and Other Centres of Luminescence

At crystal A, but not at crystals B and C, another emission range has been detected (Figure 9). Crystal A contains iron in considerable concentration

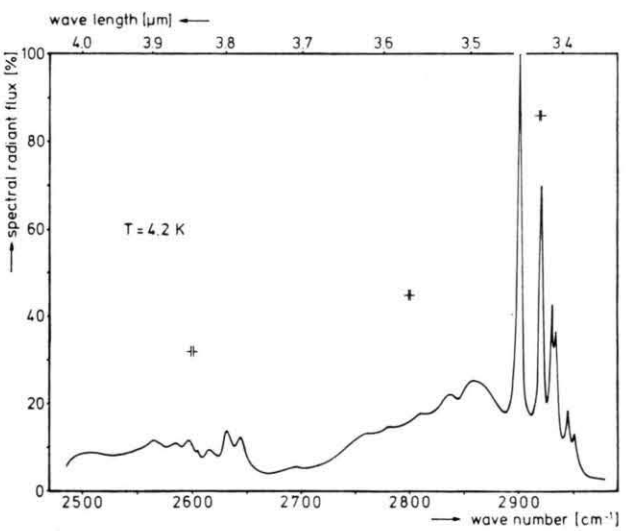

Fig. 9. Emission spectrum of Fe^{2+} centres in ZnS:Cr crystal A. Excitation range: $\bar{\nu} = 7700 \ldots 40000$ cm^{-1}. The spectrum has been corrected for the spectral response characteristics of the PbS detector.

(cf. Table 1). Similar to the findings with ZnS: Cr^{2+} emission, the i.r. emission of Fe^{2+} in ZnS [57] also shows an increasing strength in the zero phonon lines with decreasing Fe doping. In accordance with this tendency, at the investigated crystal the zero phonon lines appear more distinctly than in the mentioned paper [57]. Six sharp zero phonon lines are displayed (Table 5), the wave numbers of which are in good agreement with those in absorption at the most weakly doped ZnS: Fe crystal of [37]. The participation of vibronic bands is, in this case, particularly low.

Tab. 5. Zero phonon lines of ZnS: Fe^{2+} in emission and absorption as obtained from ZnS: Cs,Fe (crystal A).

Transition	Emission wave number (this paper, cf. Fig. 9) cm^{-1}	Absorption wave number (Slack et al. 1966 [37]) cm^{-1}
	2950.7	—
6 – 1	2945.1	2945
	2934.7	—
6 – 2	2931.3	2930
6 – 3	2921.0	2919
6 – 4	2901.3	2899

In T_d, the ^5D ground state splits into ^5E and $^5T_2$. In contrast to the d^4-configuration of Cr^{2+}, in the d^6-configuration of Fe^{2+} the ground state is ^5E. With spin-orbit interaction, the terms split further [15]: ^5E splits into five equivalent terms which are consecutively numbered [37] from 1 to 5. At low temperatures, a strong absorption is observed from $\Gamma_1(^5E)$ to $\Gamma_5(^5T_2)$ (transition 1 – 6). With higher temperatures, also the absorption transitions 2 – 6, 3 – 6, 4 – 6, and – very weakly – 5 – 6 are found.

The emission spectrum here (Fig. 9) features all these mentioned transitions – safe the transition 6 – 5 which is forbidden in T_d. The line 6 – 4, i. e. $\Gamma_5(^5T_2) \rightarrow \Gamma_5(^5E)$, is the summit of the spectrum. The emission transition 6 – 1 which was not found in [57] is but weakly pronounced due to the strong absorption 1 – 6. The satellite line at 2951 cm^{-1} could be simulated by this self-absorption. Also the transition 6 – 2 shows a satellite at 2935 cm^{-1}. In the term system of the Fe^{2+} ion in T_d symmetry the additional lines cannot be interpreted. Whereas the Γ_1 term is single, the degeneration of the threefold Γ_4 term could be removed here by a further unknown symmetry perturbation.

Due to the complexity of the zero-phonon structure, the vibronic structures in the emission spectrum (Fig. 9) are more difficult to analyse than in the case of Cr^{2+}; however, the regions of dominant coupling with acoustical or with optical modes, respectively, can clearly be distinguished.

A further emission in the spectral region $\bar{\nu} = 7000 \ldots 11000\ cm^{-1}$ is observed at crystal A (Figure 10). In the spectra at 4.2 K, sharp lines

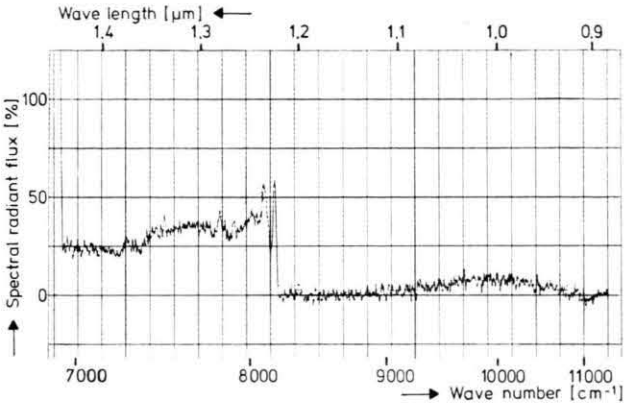

Fig. 10. Emission spectrum in the 7000 ... 11000 cm^{-1} wave number region of ZnS crystal A at $T = 4.2$ K. Excitation range: $\bar{\nu} = 18500 \ldots 40000\ cm^{-1}$.

appear at 8172 and 8095 cm^{-1}, and a third smaller maximum at 8123 cm^{-1}. Towards lower energies a broad band follows at 8030 cm^{-1}, as well as a weakly structured emission range around 7800 cm^{-1}.

At 6 K at ZnS crystals containing F-centres, a broad unstructured emission had been observed in the range from 6000 cm^{-1} to over 10000 cm^{-1} [58]. The structure of the spectrum reported here suggests, it is true, an emission within a centre. However, also with regard to the numerous impurities in crystal A, a clear association with a definite kind of centre is difficult. This is true with regard to both the emission in [58] and a luminescence near 8000 cm^{-1} which was reported [59] at 77 K. In both papers, the pertinent centres were interpreted as F-centres; the presence of F-centres in crystal A is, however, rather unlikely since this crystal was grown with excess of sulphur.

The emission of crystal A below 7000 cm^{-1} merges into a structured emission which extends down to about 5250 cm^{-1}. This emission is particularly characterized by a strong line at 6924 cm^{-1} whose position as well as the remaining structure

of the spectrum are in good agreement with the i.r. emission of cubic ZnS:Cu crystals. This agrees well with the cubic structure found at crystal A. The emission is interpreted by inner transitions in Cu^{2+} centres [60, 61].

7. Conclusions and Summary

The i.r. emission near $\bar{\nu} \approx 5000\ cm^{-1}$ of Cr doped ZnS crystals is investigated. At low temperatures, the emission spectrum is composed of two narrow zero-phonon lines at $5211\ cm^{-1}$ and $5216\ cm^{-1}$ (half widths $\Delta\bar{\nu} \approx 5\ cm^{-1}$) and of broad vibronic bands ($\Delta\bar{\nu} \geqq 50\ cm^{-1}$). By means of crystal field theory and taking into account a static Jahn-Teller effect, the lines can be interpreted as transitions within the quintet term system of the Cr^{2+} ion which is incorporated on a Zn lattice site. The T_d symmetry of the lattice site is reduced by the Jahn-Teller effect to D_{2d}. Towards smaller wave numbers, the zero phonon lines are followed by a broad structured emission range which is characterized by coupling of phonons to the electronic transitions in Cr^{2+}. From the structure of this vibronic emission spectrum which distinctly differs from the vibronic absorption spectrum it can be concluded that the participating phonons are mainly due to quasilocal vibrations involving Cr ions.

At the ZnS crystal which had the smallest Cr concentration, additional emission ranges between $2500\ cm^{-1}$ and $3000\ cm^{-1}$ and between $5250\ cm^{-1}$ and $7000\ cm^{-1}$ were found which at 4 K show the fine structure of i.r. emission of Fe^{2+} centres and of Cu^{2+} centres, respectively. With Fe^{2+}, these are the best resolved emission spectra known as yet. The transitions are interpreted in the term system of the split ^5D state of Fe^{2+} centres in T_d symmetry. A further emission in the range $\bar{\nu} = 7000 \ldots 11000\ cm^{-1}$ is detected in one sample only and cannot be assigned to a specific type of centre.

After excitation with a pulsed laser, an exponential decay curve of the Cr^{2+} i.r. emission was recorded. According to temperature the decay time constants are between 5×10^{-6} and 9×10^{-6} s. Thus, oscillator strengths of $f = 6 \times 10^{-4}$ at 4 K and $f = 10^{-3}$ at 300 K are determined. They confirm the interpretation of the i.r. emission as a parity-forbidden yet spin-allowed $^5A_1(^5E) \rightarrow {}^5B_2(^5T_2)$ transition of Cr^{2+} in D_{2d} symmetry.

Between $8000\ cm^{-1}$ and $20000\ cm^{-1}$, the excitation spectrum of the i.r. emission of Cr^{2+} centres is composed of several bands of weak intensity. In this spectral region no photoconduction is observed. The structure of the spectrum had earlier been interpreted by inner transitions to higher terms of Cr^{2+} ions: In the strong crystal field approximation using the energy matrices of Tanabe and Sugano a fit yields the crystal field parameter $Dq = 510\ cm^{-1}$ and the Racah parameters $B = 500\ cm^{-1}$, and $C = 2850\ cm^{-1}$.

Irradiation of the crystal with $\bar{\nu} \geqq 20000\ cm^{-1}$ leads to a strong excitation of the i.r. emission and to photoconduction. Between $20000\ cm^{-1}$ and $23000\ cm^{-1}$, the absorption spectrum shows a structure which is determined by transitions from Cr^{2+} centres to the conduction band. Thus, the position of the Cr^{2+} centres in the forbidden energy band can be given: At $T = 300$ K, their distance from the conduction band is $(20700 \pm 500)\ cm^{-1}$.

Electrons in the conduction band entail an excitation of the i.r. emission. Various processes are discussed which on recombination of these electrons can lead to excitation of i.r. emission. This discussion includes Cr^{3+} centres which had been introduced hypothetically by other authors. A (meta) stable existence of Cr^{3+} centres is, however, still doubtful in II-VI compounds.

By simultaneous or preceding irradiation with $\bar{\nu} \geqq 21000\ cm^{-1}$ the ZnS:Cr crystals are sensitized for excitation of the Cr^{2+} i.r. emission. Apart from an almost wave-number independent increase in the excitation spectrum which can be attributed to electron traps, a new excitation band is observed at $10500\ cm^{-1}$. The properties of this band in thermal and optical quenching experiments can be correlated with analogous e.p.r. measurements at Cr^+ centres known from literature. For an interpretation of the band, spin-forbidden transitions are suggested from the $^6A_1(^6S)$ ground state of the Cr^+ centres to the excited $^4T_1(^4G)$ term, the excited state being degenerate with conduction band states.

8. Acknowledgements

The authors wish to thank the Aerospace Research Laboratories, Wright-Patterson AFB, Ohio, for the donation of crystals, and M. Queens, Technische Hogeschool, Eindhoven, for the spectrochemical analysis. Furthermore, the support by many colleagues is gratefully acknowledged. In particular we

want to mention: absorption measurements by Dr. M. Wöhlecke and P. Wolter, the latter having carried out most of the photoconduction experiments; hospitality for some photoconduction experiments by P. Kivits and Dr. G. van der Leeden who placed his equipment at our disposal; assistance in a variety of measurements by M. Thiede and Mrs. G. Zirke; computational aid by J. Pachaly and R. Heinze; plotting of data by Miss C. Gonschor. Last not least, our thanks are extended to Miss L. Lambert for close collaboration in translating the manuscript.

To all of them we wish to express our sincere appreciation for their contributions.

[1] R. Pappalardo and R. E. Dietz, Phys. Rev. **123**, 1188 [1961].
[2] J. Dieleman, R. S. Title, and W. V. Smith, Phys. Letters **1**, 334 [1962].
[3] G. W. Ludwig and M. R. Lorenz, Phys. Rev. **131**, 601 [1963].
[4] R. S. Title, Phys. Rev. **133**, A 1613 [1964].
[5] T. L. Estle, G. K. Walters, and M. DeWit, Paramagnetic Resonance, Proc. 1st Int. Conf., Editor: W. Low, Acad. Press, New York 1963, Vol. 1, page 144.
[6] M. De Wit, A. R. Reinberg, W. C. Holton, and T. L. Estle, Bull. Amer. Phys. Soc. **10**, 329 [1965].
[7] J. T. Vallin, G. A. Slack, S. Roberts, and A. E. Hughes, Phys. Rev. B **2**, 4313 [1970].
[8] K.-D. Pautz, Diplomarbeit TU Berlin 1968.
[9] H. Gobrecht, H. Nelkowski, and G. Grebe, Verhandl. DPG [6] **4**, 159 [1969].
[10] H. Nelkowski and G. Grebe, J. Luminescence **1/2**, 88 [1970].
[11] C. S. Kelley and F. Williams, Phys. Rev. B **2**, 3 [1970].
[12] G. Grebe and H.-J. Schulz, Verhandl. DPG [6] **6**, 722 [1971].
[13] J. D. Dunitz and L. E. Orgel, J. Phys. Chem. Solids **3**, 20 [1957].
[14] M. D. Sturge, Solid State Physics **20**, 91 [1967].
[15] W. Low and M. Weger, Phys. Rev. **118**, 1119, **120**, 2277E [1960].
[16] R. E. Trees, Phys. Rev. **82**, 683 [1951].
[17] A. Filler, Diplomarbeit FU Berlin 1970.
[18] P. Wolter, Diplomarbeit TU Berlin 1973.
[19] J. T. Vallin and G. D. Watkins, Solid State Comm. **9**, 953 [1971].
[20] J. L. Prather, Atomic Energy Levels in Crystals, Nat. Bur. Standards, Monograph 19, Washington 1961.
[21] F. S. Ham, Electron Paramagnetic Resonance, Editor: S. Geschwind, Plenum Press, New York 1972, page 1.
[22] K. Kunc, M. Balkanski, and M. Nusimovici, Phys. Stat. Sol. **41**, 491 [1970].
[23] Y. Tanabe and S. Sugano, J. Phys. Soc. Japan **9**, 753, 766 [1954].
[24] G. Grebe and H.-J. Schulz, Phys. Stat. Sol. (b) **54**, K 69 [1972].
[25] J. M. Langer and J. M. Baranowski, Phys. Stat. Sol. (b) **44**, 155 [1971].
[26] P. A. Slodowy and J. M. Baranowski, Phys. Stat. Sol. (b) **49**, 499 [1972].
[27] E. M. Wray and J. W. Allen, J. Phys. C (Solid St. Phys.) **4**, 512 [1971].
[28] M. A. Catalan, F. Rohrlich, and A. G. Shenstone, Proc. Roy. Soc. London A **221**, 421 [1954].
[29] J. S. Griffith, The Theory of Transition-Metal Ions, University Press, Cambridge 1964, 2nd ed.
[30] H. L. Schläfer and G. Gliemann, Einführung in die Ligandenfeldtheorie, Akad. Verlagsges., Frankfurt 1967.
[31] O. Matumura, J. Phys. Soc. Japan **14**, 108 [1959].
[32] J. C. Phillips, Rev. Mod. Phys. **42**, 317 [1970].
[33] S. Sugano, Y. Tanabe, and H. Kamimura, Multiplets of Transition-Metal Ions in Crystals, Acad. Press, New York 1970.
[34] W. E. Hagston, J. Phys. C (Solid St. Phys.) **1**, 810 [1968].
[35] C. A. Bates, Phys. Letters A **29**, 252 [1969].
[36] B. DiBartolo, Optical Interactions in Solids, John Wiley, New York 1968.
[37] G. A. Slack, F. S. Ham, and R. M. Chrenko, Phys. Rev. **152**, 376 [1966].
[38] J. W. Allen, J. Phys. C (Solid St. Phys.) **2**, 1077 [1969].
[39] J. M. Langer, Phys. Stat. Sol. (b) **47**, 443 [1971].
[40] C. J. Ballhausen, Introduction to Ligand Field Theory, McGraw-Hill, New York 1962.
[41] H. A. Weakliem, J. Chem. Phys. **36**, 2117 [1962].
[42] J. W. Allen, Physics of Semiconductors, Proc. 7th Int. Conf., Dunod, Paris 1964, p. 781.
[43] K. Morigaki, J. Phys. Soc. Japan **19**, 187 [1964].
[44] R. Rai, J. Y. Savard, and B. Tousignant, Phys. Letters A **25**, 443 [1967].
[45] R. Rai, J. Y. Savard, and B. Tousignant, Can. J. Phys. **47**, 1147 [1969].
[46] L. Jastrzebski and J. M. Baranowski, Phys. Stat. Sol. (b) **58**, 401 [1973].
[47] P. Jaszczyn-Kopec, J. Gallagher, H. Kallmann, and B. Kramer, Phys. Rev. **140**, A 1309 [1965].
[48] T. Taki and H. Bo, J. Phys. Soc. Japan **25**, 1324 [1968].
[49] H. Schoembs, Diplomarbeit TU Berlin 1971.
[50] R. S. Title, Phys. Rev. **131**, 623 [1963].
[51] H. D. Fair, R. D. Ewing, and F. E. Williams, Phys. Rev. **144**, 298 [1966].
[52] B. Lambert, T. Buch, and P. Jaszczyn–Kopec, C. R. Acad. Sci. Paris B **271**, 1232 [1970].
[53] J. Dietrich, Diplomarbeit TU Berlin 1970.
[54] M. D. Sturge, H. J. Guggenheim, and M. H. L. Pryce, Phys. Rev. B 2, 2459 [1970].
[55] H.-E. Gumlich and H.-J. Schulz, J. Phys. Chem. Sol. **27**, 187 [1966].
[56] A. Cingolani and A. Levialdi, Phys. Rev. **158**, 732 [1967].
[57] G. A. Slack and B. M. O'Meara, Phys. Rev. **163**, 335 [1967].
[58] K. Leutwein, A. Räuber, and J. Schneider, Solid State Comm. **5**, 783 [1967].
[59] F. J. Bryant and P. S. Manning, Solid State Comm. **10**, 501 [1972].
[60] I. Broser, H. Maier, and H.-J. Schulz, Phys. Rev. **140**, A 2135 [1965].
[61] H.-J. Schulz, Festkörperprobleme **7**, Herausgeber: O. Madelung, S. 75 (1967).